JOURNAL OF THERMOPHYSICS AND HEAT TRANSFER
Vol. 7, No. 1, Jan.-March 1993

Effect of Thermal Radiation on Transient Combustion of a Fuel Droplet

Takeo Saitoh*
Tohoku University, Sendai, 980, Japan
Kouji Yamazaki†
INAX Corporation, 3-77 Minatomachi Tokoname, 479, Japan
and
Raymond Viskanta‡
Purdue University, West Lafayette, Indiana 47907

The effect of radiation heat transfer on transient combustion of a fuel droplet with a finite rate of chemical reaction and variable properties has been studied under the assumption of spherical symmetry. Evaporation curves, transient variation of flame location, temperature profiles, and the ratio of the flame to droplet radius were compared to previously published results without the radiation effect. It was found that the radiation reduces by at least 25% the maximum flame temperature. Furthermore, the present results were compared to the experimental data of several researchers. As a consequence, it was shown that the reason for the previous discrepancy between the theory and experiment was attributed to the radiation.

Nomenclature

A_{ij} = coefficient defined by Eq. (45)
a = thermal diffusivity
a^+ = a/a_∞
C_i, C_{ij} = Sutherland constant
C_p = specific heat at constant pressure
D_i = diffusion coefficient of species i
D_{ij} = mutual diffusion coefficient
D_1 = Damköhler number, $\kappa\rho_e\nu_1^0\nu_1^f R_0^2/(a_e m)$
E = activation energy
E_b = blackbody emitted flux
E_n = exponential integral function defined by Eq. (36)
G = incident radiation
g_1, g_2 = functions defined by Eqs. (29) and (30)
H_i^0 = standard heat of formation per mole of species i
$I_{b\lambda}$ = spectral blackbody radiation intensity
I_λ = spectral radiation intensity
J_1, J_2 = functions defined by Eqs. (32) and (33)
K = function defined by Eq. (31)
k = thermal conductivity
k^+ = k/k_∞
L = latent heat of vaporization
L_{ei} = Lewis number of species i, D_i/a
m_i = molecular weight of species i
n_λ = refractive index
P_a = atmospheric pressure
P_c = critical pressure
p = pressure
q_R = radiative heat flux
R^0 = universal gas constant
R_0 = initial droplet radius
R_v^0 = gas constant of fuel vapor
$R(t)$ = droplet radius
r = radial coordinate
r_f = flame-front radius
S = distance
s, s' = vector of direction
T = temperature
T_b = boiling point
T_c = critical temperature
T_e = ambient temperature
T_m = maximum flame temperature
T_r = reduced temperature
t = time
t_R = lifetime
t^+ = Fourier number defined by equation (17)
v = gas velocity in the radius direction
v_w = ejection velocity
X = transformed coordinate, Eq. (18)
Y_i = concentration of species i
y_i = molar fraction
β = extinction coefficient
Δh_c = heat of combustion of fuel per mole
δ = Stefan-Boltzmann constant
η = transformed coordinate, Eq. (19)
θ = temperature inside the droplet
κ = absorption coefficient or frequency factor
κ_P = Planck mean-absorption coefficient
μ = viscosity
ν_1^i, ν_2^j = stoichiometric coefficients of the reactant i and the product j, respectively
ξ = integration variable
ξ^* = $(\xi^2 - \tau_1^2)^{1/2}$
$\sigma_{s\lambda}$ = scattering coefficient
τ = optical radial distance
τ_0 = representative optical radial distance
Ω, Ω' = solid angle
$\dot{\omega}$ = rate of production by chemical reactions
ω_λ = single scattering albedo, $\sigma_{s\lambda}/(\sigma_{s\lambda} + K_\lambda)$

Subscripts and Superscripts

$+$ = dimensionless quantity
e, 2, ∞ = value at infinity
ℓ = droplet
w, 1 = droplet surface
i = ingredients, f fuel, o O_2, c CO_2, h H_2O, n N_2

Received Sept. 16, 1991; revision received Jan. 8, 1992; accepted for publication Jan. 14, 1992. Copyright © 1991 by the American Institute of Aeronautics and Astronautics, Inc. All rights reserved.

*Professor, Department of Aeronautics and Space Engineering.

†Researcher, Division of Equipment Development.

‡Professor, School of Mechanical Engineering.

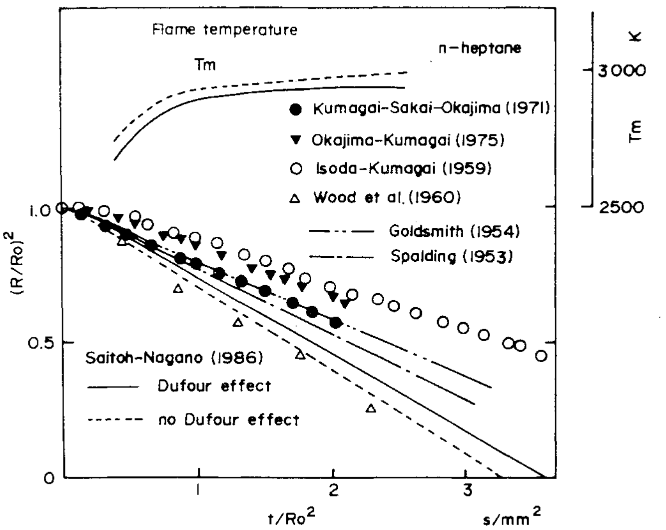

Fig. 1 Comparison of the theoretical results with experimental data.[21,22,24,33,35]

Introduction

THE importance of droplet combustion lies in the fact that it contributes to the understanding of the practical fuel spray combustion in furnaces, Diesel engines, and other combustors. Such studies are also important in the lean pre-evaporative and premixed combustion in the gas turbine combustor for aircrafts. Numerous theoretical and experimental studies on the transient droplet combustion have been reported.[34] The spray combustion includes a number of complicated processes, and an understanding of the mechanism is not complete. As a first step, an analysis of the transient combustion of a single fuel droplet has been carried out.

The present article reports on a numerical study of transient combustion of a single fuel droplet with the emphasis being placed on the effect of thermal radiation. Most earlier theoretical investigations were based on the so-called quasisteady approximation.[20,25,28] However, transient analyses by Kotake and Okazaki,[1] Hubbard et al.,[2] and Saitoh and Nagano[3] pointed out that the quasisteady analysis is invalid. Later, other effects including variable physical property, first order thermal diffusion, viscous dissipation, and natural convection,[29,30] were examined in detail by Saitoh and Nagano.[4] Among these it was found that transient, variable physical property, and natural convection effects are quite important and should not be neglected.[32]

A transient solution of droplet combustion and evaporation with variable physical properties and finite chemical reaction rate was obtained by Saitoh and Nagano.[4,5] According to their calculations (see Fig. 1), T_m is about 2300–2500 K, which is not possible in the real-droplet combustion. A comparison of numerical results with the experimental data of Okajima and Kumagai[6] (marked by symbol ▼) which is presently considered to be the most reliable for the droplet radius squared reveals that they are not in good agreement. Therefore, some other effects which have a major influence on the flame structure remain to be determined.

Motivated by the above evidence we have carried out a transient numerical analysis of droplet combustion, by accounting for thermal radiation from the flame under the considered thermophysical property variation with temperature and composition, as well as the finite rate of chemical reaction. It seems that the effect of radiation on combustion and evaporation of a fuel droplet is very important, particularly at elevated pressure[26,27] and under low gravity.

Governing Equations

Mass, Energy, and Species Conservation Equations

A fuel droplet of radius R_0 and initially at temperature T_e is ignited and a flame front at position $r = r_f$ is formed in an unbounded oxidizing environment of temperature T_e at P_a (Fig. 2). The location where the temperature is almost constant is considered to be at infinity.

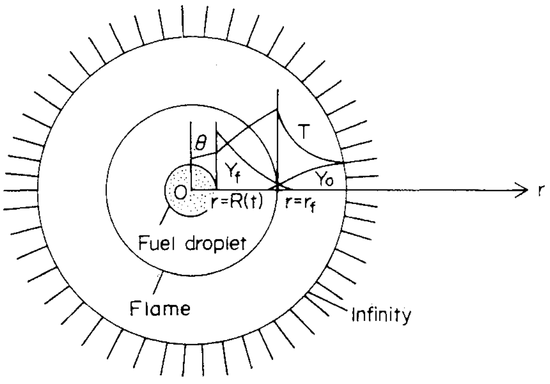

Fig. 2 Schematic model for transient burning of a single fuel droplet with radiation effect.

For the purpose of analysis, the following assumptions and idealizations are made[4]: 1) spherical symmetry; 2) pressure is constant and at atmospheric pressure in the relevant field; 3) Dufour-Soret and viscous dissipation effects are negligible; 4) convection in the liquid phase is negligible in comparison to diffusion; and 5) reaction obeys a single-step Arrhenius second-order equation.

The governing equations for the present model under the assumptions and idealizations listed above are:

Liquid Phase: $r < R(t)$

$$\frac{\partial \theta}{\partial t} = a_l \frac{1}{r^2}\frac{\partial}{\partial r}\left(r^2 \frac{\partial \theta}{\partial r}\right) \tag{1}$$

Gas Phase: $r > R(t)$

$$\frac{\partial \rho}{\partial t} + \frac{1}{r^2}\frac{\partial}{\partial r}(r^2 \rho v) = 0 \tag{2}$$

$$\rho C_p \frac{\partial T}{\partial t} + \rho C_p v \frac{\partial T}{\partial r} = \frac{1}{r^2}\frac{\partial}{\partial r}\left[r^2\left(k\frac{\partial T}{\partial r} - q_R\right)\right] + \sum_{i=0}^{n} H_i^0 \dot{\omega} \tag{3}$$

$$\rho \frac{\partial Y_i}{\partial t} + \rho v \frac{\partial Y_i}{\partial r} = \frac{1}{r^2}\frac{\partial}{\partial r}\left(\rho D_i r^2 \frac{\partial Y_i}{\partial r}\right) + (\nu_2^i - \nu_1^i) m_i \dot{\omega} \tag{4}$$

$$p = \rho R^0 T \sum_{i=0}^{n} \frac{Y_i}{m_i} \tag{5}$$

The radial flow velocity v can be obtained by solving the continuity Eq. (2) instead of the momentum equation. The reaction term $\dot{\omega}$ in Eqs. (3) and (4) is given by the following single-step Arrhenius second-order equation:

$$\dot{\omega} = \frac{\kappa \rho^2 Y_o Y_f}{m_0 m_f} \exp\left(-\frac{E}{R^0 T}\right) \tag{6}$$

The boundary conditions for these equations are[7]

Initial Condition:

$$t = 0: \quad \theta = T_e \qquad 0 \le r \le R_0 \tag{7}$$

$$T = T_0(r),\ Y_i = Y_{ie}(r) \qquad r > R_0 \tag{8}$$

Boundary Condition:

$$r = 0: \qquad \frac{\partial \theta}{\partial r} = 0 \tag{9}$$

$$r = \infty: \qquad Y_f = 0, \quad Y_o = Y_{oe}, \; T = T_e \tag{10}$$

Coupling Condition at Droplet Surface:

$$r = R(t): \qquad -\rho D_f \frac{\partial Y_f}{\partial r} = \rho v_w (1 - Y_{fw}) \tag{11}$$

$$\rho D_o \frac{\partial Y_o}{\partial r} = \rho v_w Y_{ow} \tag{12}$$

$$v_w = \frac{\mathrm{d}R}{\mathrm{d}t}\left(1 - \frac{\rho_l}{\rho}\right) \tag{13}$$

$$\rho_l L \frac{\mathrm{d}R}{\mathrm{d}t} = k_l \frac{\partial \theta}{\partial r}\bigg|_- - k \frac{\partial T}{\partial r}\bigg|_+ + q_R \tag{14}$$

$$Y_{fw} = \exp\left[-\frac{L}{R_v^0 T_b}\left(\frac{T_b}{T_w} - 1\right)\right] \tag{15}$$

$$\theta|_- = T|_+ \tag{16}$$

Since the pressure is assumed to be atmospheric pressure throughout the relevant field, the Clausius-Clapeyron's relation of phase transformation can be applicable.

Next, we introduce the following dimensionless variables:

$$r^+ = \frac{r}{R_0}, \quad t^+ = \frac{at}{R_0^2}, \quad (T^+, \theta^+) = \frac{C_p \alpha_f}{\Delta h_c}(T, \theta)$$

$$Y_i^+ = \alpha_i Y_i, \quad \alpha_i = -\frac{m}{(\nu_2^i - \nu_1^i) m_i}, \quad v^+ = \frac{R_0}{a} v$$

$$m = \sum \nu_1^i m_1 = \sum \nu_2^i m_2, \quad \Theta = \frac{E}{R^0} \cdot \frac{C_p \alpha_f}{\Delta h_c}$$

$$R^+(t^+) = \frac{R(t)}{R_0}, \quad q_R^+ = \frac{\alpha_f R_0 q_R}{\rho a \Delta h_c} \tag{17}$$

In order to immobilize the moving interface the following boundary fixing method is used.[8,31]

Liquid Phase:

$$X = \frac{r^+}{R^+(t^+)} \tag{18}$$

Gas Phase:

$$\eta = \ln\left(\frac{r^+}{R^+(t^+)}\right) \tag{19}$$

The governing equations are rewritten through the aid of the foregoing transformations and the dimensionless variables as

$$\frac{\partial \theta^+}{\partial t^+} = a_l^+ \frac{1}{R^{+2}} \frac{\partial^2 \theta^+}{\partial X^2} + \left(\frac{X\dot{R}^+}{R^+} + \frac{2}{X}\frac{a_l^+}{R^{+2}}\right)\frac{\partial \theta^+}{\partial X} \tag{20}$$

$$L[T^+, 1, 1, -1) = 0 \tag{21}$$

$$L[Y_i^+, L_{ei}, 0, 1] = 0 \tag{22}$$

Where the operator $L[\;]$ is defined by

$$L[\Omega, h, m, n) = \frac{\partial \Omega}{\partial t} - \frac{1}{hr^{+2}}\frac{\partial^2 \Omega}{\partial \eta^2} - \left(\frac{1}{hr^{+2}} + \frac{\dot{R}^+}{R^+} - \frac{v^+}{r^+}\right)$$
$$\times \frac{\partial \Omega}{\partial \eta} - \frac{m}{r^{+2}}\left(\frac{1}{r^+} + \frac{\dot{R}^+}{R^+}\right)\frac{\partial q_R^+}{\partial \eta} + nD_1 Y_0^+ Y_f^+$$
$$\times \exp\left(-\frac{\Theta}{T^+}\right) \tag{23}$$

Radiative Transfer Equations

For radiative transfer in absorbing, emitting, and scattering media, we have to consider two kinds of governing equations, i.e., transfer equation and the energy equation. The radiative transfer equation for a spherical coordinate system (see Fig. 3) under the assumption of isotropic scattering is given by Viskanta et al.[9]

$$\mu \frac{\partial I_\lambda}{\partial r} + \frac{1 - \mu^2}{r}\frac{\partial I_\lambda}{\partial \mu} = -(k_\lambda + \sigma_{s\lambda}) I_\lambda + k_\lambda I_{b\lambda}$$
$$+ \frac{\sigma_{s\lambda}}{2}\int_{-1}^{1} I(r, \mu')\,\mathrm{d}\mu' \qquad (\mu = \cos\theta) \tag{24}$$

The radiative flux divergence, the first term q_R on the right side of Eq. (3), is obtained by integrating Eq. (24) over all directions, i.e., $-1 \le \mu \le 1$

$$\frac{1}{r^2}\frac{\partial}{\partial r}(r^2 q_R) = K_p(4E_b - G) \tag{25}$$

where

$$q_R(r) = \int_{\Omega=4\pi} I(r, \mu)\,\mu\,\mathrm{d}\Omega = 2\pi \int_{-1}^{1} I(r, \mu)\mu\,\mathrm{d}\mu \tag{26}$$

$$G(r) = \int_{\Omega=4\pi} I(r, \mu)\,\mathrm{d}\Omega = 2\pi \int_{-1}^{1} I(\mathrm{r}, \mu)\,\mathrm{d}\mu \tag{27}$$

The optical radial distance[19] τ is defined as $\tau = \beta \cdot r$ and irradiance $G(r)$ can be expressed as[9]

$$G(\tau) = \frac{2}{\tau}\left[J_1 g_1(\tau) + J_2 g_2(\tau) + \int_{\tau_1}^{\tau_2} K(\tau, \xi) S(\xi)\,\mathrm{d}\xi\right] \tag{28}$$

Here

$$g_1(\tau) = \tau_1 E_2(\tau - \tau_1) - E_3(\tau - \tau_1) + E_3(\tau^*) \tag{29}$$

$$g_2(\tau) = \tau_2 E_2(\tau_2 - \tau) - E_3(\tau_2 - \tau)$$
$$- \tau_2^* E_2(\tau_2^* - \tau^*) - E_3(\tau_2^* + \tau^*) \tag{30}$$

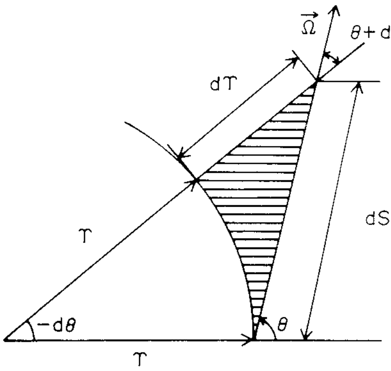

Fig. 3 Spherical coordinate system.

$$K(\tau, \xi) = [E_1(|\tau - \xi|) - E_1(|\tau^* - \xi^*|)]\cdot\xi \quad (31)$$

$$J_1 = \varepsilon_1 E_{b1} + [(1/\varepsilon_1) - 1](\varepsilon_1 E_{b1} - q_{R1}) \quad (32)$$

$$J_2 = \varepsilon_2 E_{b2} + [(1/\varepsilon_2) - 1](\varepsilon_2 E_{b2} - q_{R2}) \quad (33)$$

$$S(t) = (1 - \omega_\lambda)E_b - [\omega_\lambda G(t)/4] \quad (34)$$

$$\tau^* = (\tau^2 - \tau_1^2)^{1/2}, \quad \tau_2^* = (\tau_2^2 - \tau_1^2)^{1/2} \quad (35)$$

The exponential integral function E_n is defined as

$$E_n(\tau) = \int_0^1 \mu^{n-2}\cdot \exp\left(-\frac{\tau}{\mu}\right) \mathrm{d}\mu \quad (36)$$

In the above equations, the following assumptions and idealizations have been made[10]:

1) Scattering is negligible in comparison to absorption ($\sigma \ll \kappa$).

2) Emissivity of droplet surface and of surroundings at infinity are 1.0, and the temperatures are the boiling point and the ambient temperature, respectively.

3) The representative optical radius is small ($\tau_0 \ll 1$). Therefore, the exponential integral functions can be approximated as

$$E_2(\tau) = 1 - \mathrm{O}(\tau) \qquad E_3(\tau) = \tfrac{1}{2} - \tau + \mathrm{O}(\tau) \quad (37)$$

4) The Planck absorption coefficient κ_P is constant $\kappa_P = 0.35$.

The Planck absorption coefficient κ_P is calculated as the function of temperature and composition (concentration of CO_2 and H_2O). However, the results obtained were nearly the same as the one in which κ_P is assumed to be constant. Therefore, a constant κ_P is to generate the results reported in the article by Saitoh et al.[11]

We have assumed that the radiation stops at the droplet surface (above assumption 2). In fact it is reported in the literature that the emissivity takes the value over 0.8 if the penetration distance were larger than 200 μm.[12]

Physical Properties

The physical property value expressions in the present computations are presented in this section. It was assumed that the gas mixture consists of two components, i.e., gas and air. The concentration Y_i used in the various expressions means the mole fraction. The relation between mass and mole fraction is given by the following equations:

$$y_f = \frac{Y_f/M_f}{Y_f/M_f + Y_a/M_a} \quad (38)$$

$$y_a = 1 - y_f \quad (39)$$

The property value expressions for density ρ, C_p, μ, k, diffusion coefficient D_i, and L are summarized below[13]:

1) ρ, Density can be obtained from the equation of state of an ideal gas

$$\rho = p \sum y_i M_i/RT \qquad \text{kg/m}^3 \quad (40)$$

2) C_p

$$C_{p_i} = A + B\cdot T + C\cdot T^2 + D\cdot T^3 \qquad \text{kJ/kg}\cdot\text{mol}\cdot\text{K} \quad (41)$$

where, A, B, C, D denote the constant that is determined by substances. The constants for air and *n*-heptane are listed in Table 1.

Table 1 Constants in specific heat at constant pressure

	A	$B \times 10^{-6}$	$C \times 10^{-6}$	$D \times 10^{-9}$
n-Heptane	−7.727	676168	−365.1	76.58
O_2	25.845	−3.680	17.45	−10.65
H_2O	32.243	19238	10.55	−3.56
CO_2	19.795	7343	−56.02	17.52
N_2	31.150	−13565	26.80	−11.68

Table 2 Critical temperature, critical pressure and molecular weight

	M	T_c, K	P_c, MPa
n-Heptane	100.20	540.2	2.748
O_2	32.00	154.6	5.04
N_2	28.01	126.2	3.40
CO_2	44.01	304.2	7.38
H_2O	18.02	647.3	22.12
Air	28.97	132.5	3.77

3) μ, by virtue of the Licht-Stechert equation[14]

$$\mu_i = 13.86 \times \left(\frac{M_i^3 \times P_{ci}^4}{T_{ci}}\right)^{1/6} \frac{T_{ri}^{3/2}}{T_{ri} + 0.8} \qquad 10^{-7}\ \text{Pa}\cdot\text{s}$$

$$T_{ri} = \frac{T_i}{T_{ci}} \quad (42)$$

T_c, and P_c are shown in Table 2.

4) Thermal conductivity k, from Eucken's Equation[15]

$$k_i = \mu_i[0.1 \times C_{p_i} + (1.039/M_i)] \qquad \text{kJ/m}\cdot\text{s}\cdot\text{K} \quad (43)$$

Thermal conductivity for mixture is obtained from the Lindsay-Bromley's equation[16]

$$k_m = \sum_{i=1}^{m} \frac{k_i}{1 + \dfrac{1}{y_i}\displaystyle\sum_{\substack{j=1\\ j\neq i}}^{n} A_{ij}\cdot y_j} \qquad \text{kJ/m}\cdot\text{s}\cdot\text{K} \quad (44)$$

where

$$A_{ij} = \frac{1}{4}\left\{1 + \left[\frac{\mu_i}{\mu_j}\left(\frac{M_j}{M_i}\right)^{3/4} \frac{1 + C_i/T}{1 + C_j/T}\right]^{1/2}\right\}^2 \frac{1 + C_{ij}/T}{1 + C_i/T} \quad (45)$$

The Sutherland constants C_i, C_j and C_{ij} are given by

$$C_i = 1.47 \times T_{b_i} \qquad K \quad (46)$$

$$C_{ij} = \sqrt{C_i\cdot C_j} \qquad \text{K} \quad (47)$$

5) Diffusion coefficient D_i; Wilke's equation[17] is used to obtain the diffusion coefficient D_i

$$D_i = (1 - y_i)/\sum_{\substack{j=1\\ j\neq i}} (y_i/D_{ij}) \qquad 10^{-8}\text{m}^2/\text{s} \quad (48)$$

Where D_{ij} is given by Fujita's equation.[18]

$$D_{ij} = 0.70T^{1.833}\left[\left(\frac{T_c}{P_c}\right)_i^{1/3} + \left(\frac{T_c}{P_c}\right)_j^{1/3}\right]^{-3} \cdot\left(\frac{1}{M_i} + \frac{1}{M_j}\right)^{1/2} \qquad 10^{-8}\ \text{m}^2/\text{s} \quad (49)$$

6) Latent heat of evaporation $L(T_w)$ is approximated by the following equation:

$$L(T_w) = 55.53(T_c - T_w)^{0.3436} \qquad \text{kJ/kg} \quad (50)$$

Table 3 Liquid physical properties (*n*-heptane)

Property	*n*-Heptane
α_l	6.32×10^{-8}, m²/s
k_l	11.34×10^{-5}, kJ/msK
ρ_l	626, kg/m³

Table 4 Physical properties and pertinent data (*n*-heptane)

	Unit			Unit	
a_e	m²/s	24.86×10^{-6}	T_b	K	371.4
Cp_e	kJ/kg K	0.2366	α_f		4.513
E	kJ/mol	25	α_o		1.285
Δh_c	kJ/kg	10650	Θ		1.9273
k_e	kJ/ms K	0.692×10^{-5}	ρ_e	kg/m³	1.177
Le_f		1	Le_o		1
$L = 55.53\,(540 - T_w)^{0.3436}$ kJ/kg					

7) Properties in the liquid phase are assumed to be constant and listed in Table 3. These values were evaluated at 300 K.

Numerical Method of Solution

A fully implicit finite-difference method is employed in the numerical solution of the model equations. The fuel used is *n*-heptane. We first assume an appropriate form of the initial profiles of the temperature and concentration. The initial temperature and concentration profiles were found to be very important to obtain meaningful and stable solutions. The physical properties used in the calculations are summarized in Table 4.

Numerical Results and Discussion

Figures 4 and 5 show the typical flame structure at an intermediate time and near the end of combustion, respectively. A sharp peak in the temperature together with a narrow reaction zone shown in Fig. 4 indicate the thin flame nature. The temperature has its maximum at $\eta = 2.1$, which is about 25% lower than when thermal radiation is neglected in the energy equation.

A first glance at Figs. 4 and 5 the flame-front locations seem nearly the same, but since both figures are plotted using a transformed coordinate [Eq. (19)], actual location at time t_l (Fig. 5) is much farther than in Fig. 4. Therefore, the temperature gradient was decreased considerably. The maximum flame temperature drop is nearly equal to that at middle time stage.

Figure 6 shows time sequence of the temperature distribution. The flame front moves away from the droplet surface with time, and the maximum flame temperature increases gradually.

The spatial distribution of physical properties at the intermediate time stage is shown in Fig. 7. The thermal conductivity and thermal diffusivity have their maximum at the flame front, and depend strongly on the temperature. The specific heat at constant pressure depends more on temperature than on fuel density and has its maximum near the droplet surface. Density has its minimum at the flame front. As a result, the physical properties of the fuel change in a complicated manner with both temperature and concentration.

The time-wise variation of the droplet radius squared, flame location, and the ratio of flame to droplet radius are plotted in Fig. 8. It is evident that d^2-law holds true for the period of combustion. Consideration of radiation in the energy equation yields a smaller burning constant, i.e., large lifetime. This is due to the fact that the maximum temperature decreases in the presence of radiation. In this analysis we accounted for radiation transfer towards the droplet surface, and the ratio of conduction heat flux to radiation heat flux was approximately 3.3 : 1. Judging from the computed results of the droplet lifetime, the outward heat loss from the flame by the radiation is larger than the inward heat loss. The flame location takes a convexed curve with its maximum at $t^+ = 40$. The dimensionless r_f/R increases continuously and is a lower value than the case without radiation.

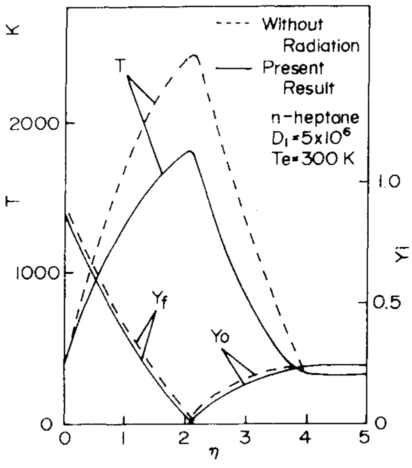

Fig. 4 Typical flame structure ($t = t_l/2$).

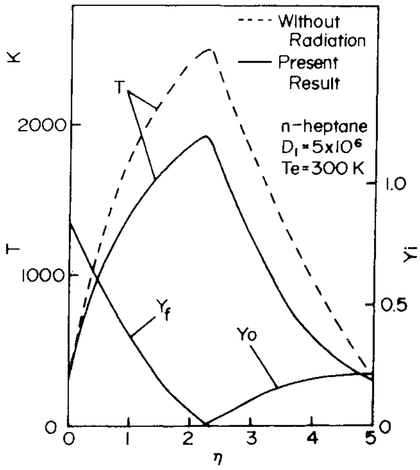

Fig. 5 Typical flame structure ($t = t_l$).

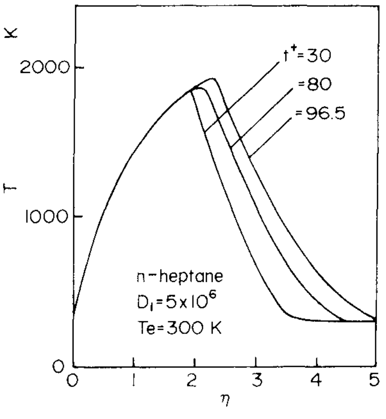

Fig. 6 Time variation of temperature profile.

A comparison of the present results with the experimental data under the zero-gravity condition is shown in Figs. 9 and 10. The present results are in better agreement with the experimental results than those obtained when radiation transfer was neglected. As far as the ratio of flame to droplet radius is concerned, the agreement is not very satisfactory, especially in the latter half of the lifetime. The results imply that further

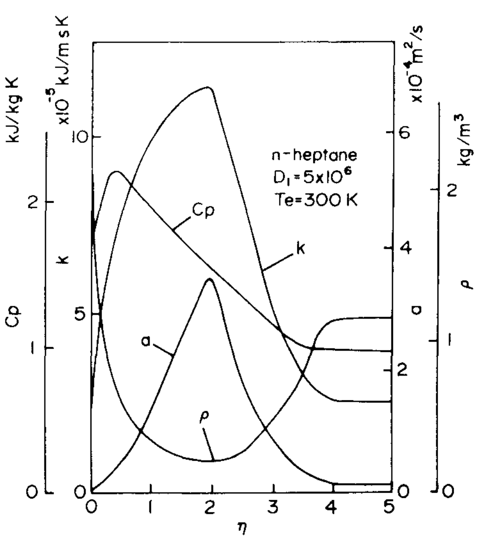

Fig. 7 Spatial distribution of physical properties ($t = t_l/2$).

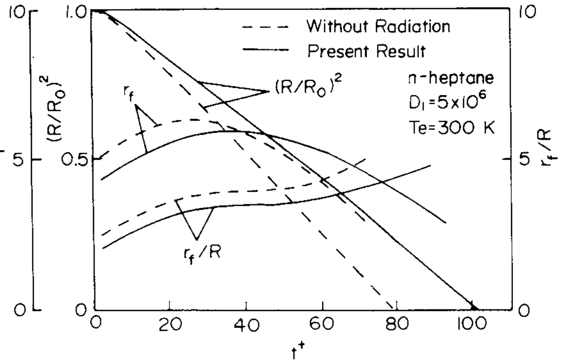

Fig. 8 Time variation of $(R/R_0)^2$, r_f, and r_f/R.

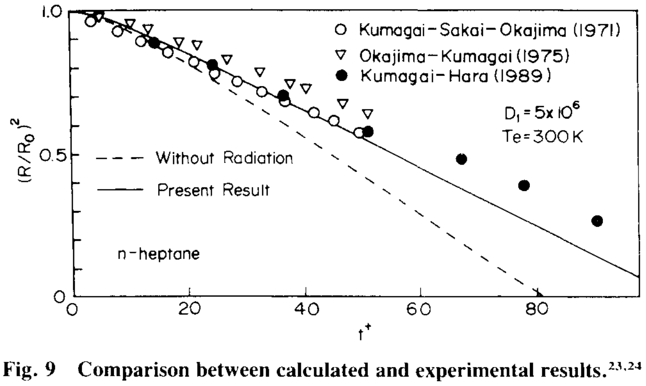

Fig. 9 Comparison between calculated and experimental results.[23,24]

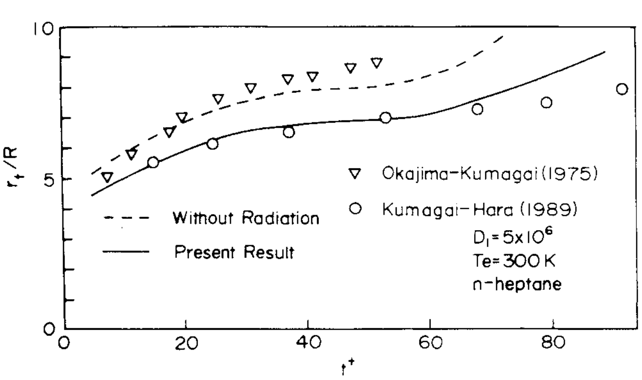

Fig. 10 Comparison between calculated and experimental results.[23]

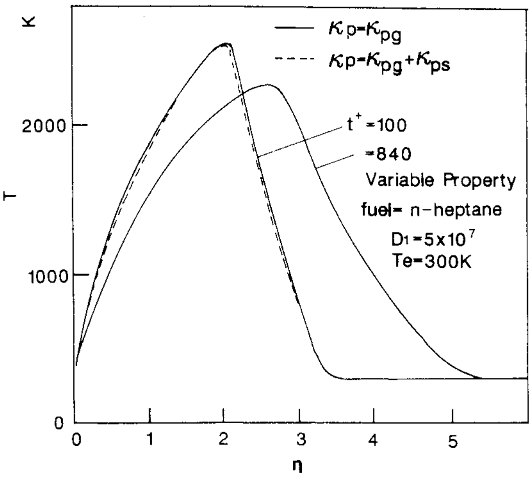

Fig. 11 Time history of temperature distribution when soot formation is considered.

investigations are required to elucidate the discrepancies between the theory and the experiment.

It is important to validate the effect of soot formation for luminous flame, e.g., *n*-heptane droplet. We considered the effect of soot formation by accounting for increase of absorption coefficient between the droplet surface and the soot location.

As a result, the total absorption coefficient κ_p can be represented as the sum of absorption coefficients of gas κ_{p_g} and soot κ_{p_s}. Fig. 11 indicates the result of calculation showing the effect of soot formation.

A broken line shows the case in which the soot formation effect was considered. A comparison between the two reveals that the soot formation does not alter the entire temperature profile, at least in the range of pressure considered.

Concluding Remarks

The following conclusions can be drawn from the present transient numerical analysis for combustion of a spherical fuel droplet, which takes account of chemical reaction, variable properties, and thermal radiation:

1) Thermal radiation has a significant influence on droplet combustion. For a *n*-heptane droplet, the decrease of the maximum flame temperature amounts to at least 25%.

2) The physical properties change drastically with temperature and concentration, and have a significant effect on the droplet combustion.

3) Comparison of the present results with the experimental data reveals that the droplet radius squared and the ratio flame to droplet radius are in good agreement, while the ratio of flame to droplet still tends to deviate from the experimental data in the latter half of the lifetime.

In closing, further investigations should be conducted on the effect of radiation during fuel combustion at elevated pressure.

Acknowledgments

The authors extend sincere thanks to E. Nakata for great assistance in preparing this article.

References

[1] Kotake, S., and Okazaki, T., "Evaporation and Combustion of a Fuel Droplet," *International Journal of Heat and Mass Transfer*, Vol. 12, No. 5, 1969, pp. 595–609.

[2] Hubbard, G. L., Denney, V. E., and Mills, A. F., "Droplet Evaporation: Effect of Transients and Variable Properties," *International Journal of Heat and Mass Transfer*, Vol. 18, Nos. 7 and 8, 1975, pp. 1003–1008.

[3] Saitoh, T., and Nagano, O., "Transient Combustion of a Fuel Droplet with Finite Rate of Chemical Reaction," *Combustion Science and Technology*, Vol. 22, No. 8, 1980, pp. 227–234.

[4] Saitoh, T., and Nagano, O., "Transient Behavior of Combustion and Evaporation of a Fuel Droplet with Finite Rate of Chemical Reaction and Variable Properties," TR, Tohoku Univ., Vol. 51, No. 2, 1986, pp. 129–141.

[5] Saitoh, T., and Nagano, O., "Transient and Variable Property Analysis for Droplet Evaporation," TR, Tohoku Univ., Vol. 49, No. 1, 1984, pp. 29–43.

[6] Okajima, S., and Kumagai, S., "Further Investigation of Combustion of Fuel Droplets in a Freely Falling Chamber Including Moving Droplets," *Proceedings of the Fifteenth Symposium (International) on Combustion*, Combustion Inst., Tokyo, 1975, pp. 401–407.

[7] Viskanta, R., and Mengüç, M. P., "Radiation Heat Transfer in Combustion Systems," *Progress in Energy and Combustion Science*, Vol. 14, No. 2, 1987, pp. 97–160.

[8] Saitoh, T., "Numerical Method for Multi-Dimensional Freezing Problems in Arbitrary Domains," *Journal of Heat Transfer*, Vol. 100, No. 2, 1978, pp. 294–299.

[9] Viskanta, R., and Merriam, R. L., "Heat Transfer by Combined Conduction and Radiation Between Concentric Spheres Separated by Radiating Medium," *Journal of Heat Transfer*, Vol. 90, No. 2, 1968, pp. 248–256.

[10] Negrelli, D. E., Lloyd, J. R., and Novotny, J. L., "A Theoretical and Experimental Study of Radiation-Convection Interaction in a Diffusion Flame," *Journal of Heat Transfer*, Vol. 99, No. 2, 1977, pp. 212–220.

[11] Saitoh, T., and Yamazaki, K., "Effect of Thermal Radiation Transient Combustion of a Fuel Droplet with a Finite Rate of Chemical Reaction," *Proceedings of the Twenty-Seventh National Symposium on Combustion*, Japanese Combustion Society, Fuknoka, Japan, 1989, pp. 486–488.

[12] Goldsmith, A., Waterman, T. E., and Hirschhorn, J. J., *Handbook of Thermophysical Properties of Solid*, Vols. 1–5, Pergamon, Oxford, England, UK, 1961.

[13] Sato, K., *Evaluation Methods for Property Values*, Maruzen, Tokyo, 1975.

[14] Licht, W., and Stechert, D. G., Jr., "The Variation of the Viscosity of Gases and Vapors with Temperature," *Journal of Physical Chemistry*, Vol. 48, No. 1, 1944, pp. 23–47.

[15] Eucken, A., "Allgemeine Gesetzmäßigkeiten für das Wärmeleitirermögen verschiedener Stoffarten und Aggregatzustände," *Forschung*, Vol. 11, No. 1, 1940, pp. 6–20.

[16] Lindsay, A. L., and Bromley, L. A., "Thermal Conductivity of Gas Mixtures," *Industrial Engineering and Chemistry*, Vol. 42, No. 8, 1950, pp. 1508–1511.

[17] Wilke, C. R., "Diffusional Properties of Multicomponent Gases," *Chemical Engineering Progress*, Vol. 46, No. 2, 1950, pp. 95–104.

[18] Fujita, S., "Coefficients of Diffusion in Gaseous Systems," *Chemical Engineering*, Vol. 15, No. 5, 1951, pp. 234–236.

[19] Abu-Romia, M. M., and Tien, C. L., "Appropriate Mean Absorption Coefficients for Infrared Radiation Gases," *Journal of Heat Transfer*, Vol. 89, No. 4, 1967, pp. 321–327.

[20] Godsave, G. A. E., "Studies of the Combustion of Drops in a Fuel Spray—The Burning of the Single Drops of Fuel," *Proceedings of the Fourth Symposium (International) on Combustion*, Williams and Wilkins, MA, 1953, pp. 818–830.

[21] Goldsmith, M., and Penner, S. S., "On the Burning of Single Drops of Fuel in an Oxidizing Atmosphere," *Jet Propulsion*, Vol. 24, No. 4, 1954, pp. 245–251.

[22] Isoda, H., and Kumagai, "New Aspects of Droplet Combustion," *Proceedings of the Seventh Symposium (International) on Combustion*, Combustion Inst., London and Oxford, 1959, pp. 523–531.

[23] Hara, H., and Kumagai, S., "Experiment on Combustion of a Fuel Droplet Under Micro-Gravity Condition," *Proceedings of the Twenty-Seventh National Symposium on Combustion*, Japanese Combustion Society, Fuknoka, Japan, 1989, pp. 480–482.

[24] Kumagai, S., Sakai, T., and Okajima, S., "Combustion of Free Fuel Droplets in a Freely Falling Chamber," *Proceedings of the Thirteenth Symposium (International) on Combustion*, Combustion Inst., Salt Lake City, UT, 1971, pp. 779–785.

[25] Law, C. K., "Quasi-Steady Droplet Vaporization Theory with Property Variation," *Physics of Fluids*, Vol. 18, No. 11, 1975, pp. 1426–1432.

[26] Niioka, T., and Sato, J., "Combustion and Microexplosion Behavior of Miscible Fuel Droplets under High Pressure," *Proceedings of the Twenty-First Symposium (International) on Combustion*, Combustion Inst., Munich, Germany, 1986, pp. 625–631.

[27] Niioka, T., and Tsukamoto, T., "Numerical Simulation of Fuel Droplet Combustion under High Pressure," *Proceedings of the Japan/Australia Joint Meeting*, 1989, pp. 11–13.

[28] Ragfunandan, B. N., and Mukunda, H. S., "The Problem of Liquid Droplet Combustion—A Re-Examination," *Combustion and Flame*, Vol. 30, No. 1, 1977, pp. 71–84.

[29] Saitoh, T., and Sasaki, N., "Unsteady Analysis for Evaporation of Single Liquid Droplet," *Proceedings of the Fifteenth National Heat Transfer Symposium*, Sappora, Japan, 1977, pp. 286–288.

[30] Saitoh, T., and Sasaki, N., "Two-Dimensional Analysis of Combustion of Fuel Droplet or Sphere Under Conditions of Natural Convection," *Transactions of the Japan Society of Mechanical Engineers*, Vol. 50, No. 453, 1984, pp. 1397–1402.

[31] Saitoh, T., *Computer-Aided Heat Transfer,* Youkendo, Tokyo, 1986.

[32] Saitoh, T., "Recent Status of Fuel Droplet Combustion," *Journal of the Japan Combustion Society*, Vol. 87, 1991, pp. 17–36.

[33] Spalding, D. B., "The Combustion of Liquid Fuels," *Proceedings of the Fourth Symposium (International) on Combustion*, Williams and Wilkins, MA, 1953, pp. 847–864.

[34] Wise, H., Lorrel, J., and Wood, B. J., "The Effect of Chemical and Physical Parameters on Burning Rate of a Liquid Droplet," *Proceedings of the Fifth Symposium (International) on Combustion*, Combustion Inst., Pittsburgh, PA, 1955, pp. 132–141.

[35] Wood, B. J., Wise, H., and Inami, S. H., "Heterogeneous Combustion of Multicomponent Fuels," *Combustion and Flame*, Vol. 36, No. 3, 1960, pp. 235–242.